Pergamon

SCIENCE DIRECT®

Bioorganic & Medicinal Chemistry 11 (2003) 1363–1369

BIOORGANIC & MEDICINAL CHEMISTRY

Complementary Characteristics of Homologous *p*-Octiphenyl β-Barrels with Ion Channel and Esterase Activity

Abhigyan Som, Naomi Sakai and Stefan Matile*

Department of Organic Chemistry, University of Geneva, CH-1211 Geneva 4, Switzerland

Received 14 May 2002; accepted 22 November 2002

Abstract—We report that decreasing β-sheet length in homologous multifunctional rigid-rod β-barrels with internal histidines increases ion channel stability by three orders of magnitude, reduces binding activity by four orders of magnitude, and reduces esterase activity up to 22-times. These results are further used to evaluate methods employed to characterize suprastructure and activity of synthetic multifunctional pores formed by *p*-octiphenyl β-barrels with emphasis on applicability of the Hille model to determine internal diameters and the Woodhull equation to locate internal active sites.

Introduction

The prospect of anisotropic catalysis within the transmembrane confined space provided by synthetic ion channels has attracted our attention because spatial compartmentalization by the surrounding bilayer membrane introduces, *in principle*, vectorial control over substrate addition and detectability of chemical reactions at the single-molecule level.[1–5] A first attempt to synthesize a 'catalytic ion channel' was made with rigid-rod β-barrel **1** (Fig. 1).[1,6] We identified that supramolecule **1** has indeed substantial ion channel and esterase activity. The stability of ion channel **1** was, however, insufficient for practical applications in single-molecule catalysis. In the hope to stabilize *p*-oligophenyl β-barrels with ion channel and esterase activity, we decided to make and study homologous tetramer **2**.[6] In rigid-rod β-barrel **2**, *p*-octiphenyl staves are tied together with eight-stranded β-sheets formed by interdigitating tripeptide strands of the sequence LHL, while *p*-octiphenyl β-barrel **1** comprises the homologous LHLHL-pentapeptides. We here report that barrel contraction by this β-sheet truncation converts superb esterases but poor ion channels **1** into poor esterases but excellent ion channels **2**.

Results and Discussion

Monomeric *p*-octiphenyl $\mathbf{2}^{m}$ was synthesized following the procedure reported for homologue $\mathbf{1}^{m}$.[1] Ion channel activity of β-barrel **2** was studied in planar lipid bilayers composed of fresh egg yolk phosphatidylcholine (EYPC-BLMs) at pH 5.0.[1] Single ion channels that remain open for seconds were detectable in presence of β-barrel **2** (Fig. 2). As for ion channels of high stability formed by *p*-octiphenyl β-barrels with internal lysines,[7] contracted β-barrel **2** was quite difficult to characterize because of the rare occurrence of 'on-off' transitions. Comparison with the short lifetime of homologue **1** suggested that β-sheet truncation in homologue **2** stabilizes *p*-octiphenyl β-barrels by a factor of 1000 (Table 1).[8]

Ion channels formed by labile homologue **1** and stable homologue **2** exhibited ohmic behavior (Fig. 3). Consistent with the expected smaller inner diameter, the magnitude of the single-channel conductance $g = 0.7$ nS of **2** was 57% of that observed for expanded homologue **1**.

Assuming ion channels as electrolyte filled cylinders, their diameter d can be estimated from ion channel conductance g with Hille's model

Abbreviations: CB, Cascade Blue = Pyrenyl-8-X-oxy-1,3,6-trisulfonate; EYPC, Egg yolk phosphatidylcholine; *G*: $-OCH_2CO-$, H-*G*-OH, glycolic acid; H, L-Histidine = His; HPTS, 8- Hydroxypyrene-1,3,6-trisulfonate; L, L-Leucine = Leu; MeIm, 4(5)-Methylimidazole; MES, 2-Morpholinoethanesulfonic acid monohydrate; SUVs, Small unilamellar vesicles.

*Corresponding author. Tel.: +41-22-702-6085; fax: +41-22-328 7396; e-mail: stefan.matile@unige.ch

0968-0896/03/$ - see front matter © 2003 Elsevier Science Ltd. All rights reserved.
doi:10.1016/S0968-0896(02)00620-X

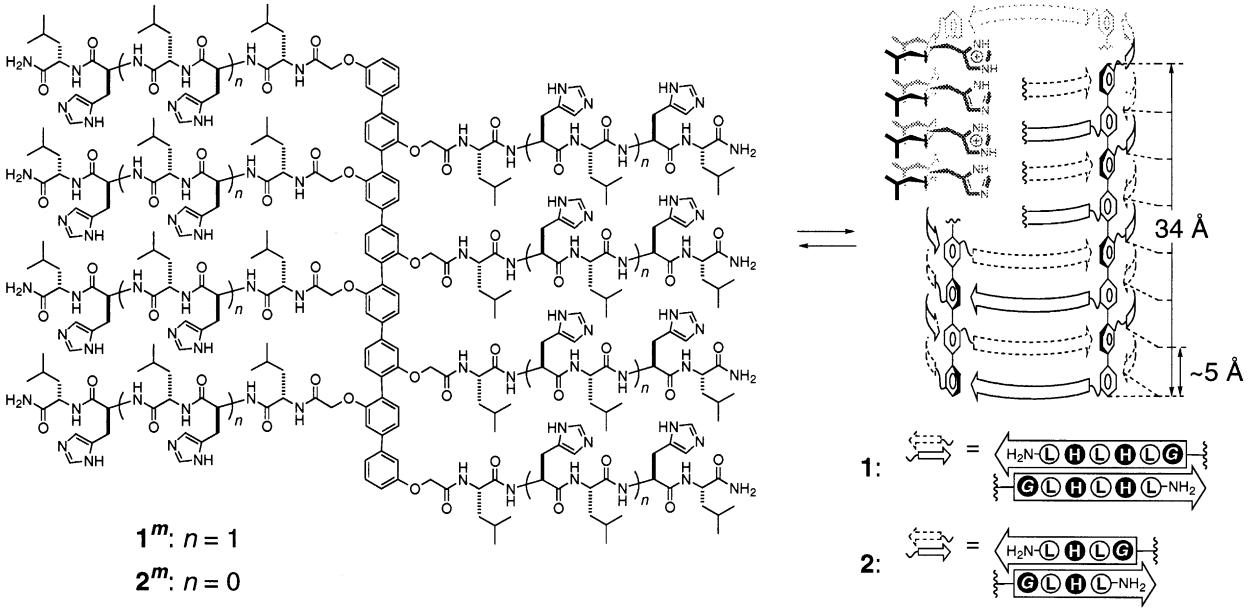

Figure 1. Self-assembly of homologous *p*-octiphenyls **1**^{m} and **2**^{m} into homologous *p*-octiphenyl β-barrels **1** and **2**, depicted as schematic cutaway suprastructure with vertical distances estimated from molecular models,[12] β-strands as arrows pointing to the C-terminus, external α-hydroxy and α-amino acid residues (one-letter abbreviation, *G*: –OCH_2CO–) black on white and internal ones white on black.

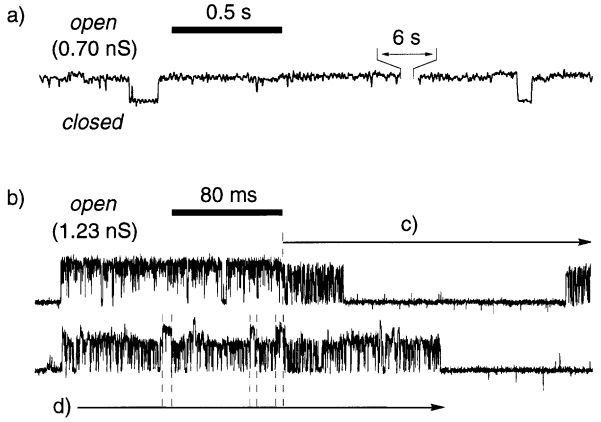

Figure 2. Typical single-channel currents for homologous ion channels **2** (a) and **1** (b) at −25 mV in EYPC-BLMs (33 mg EYPC / mL *n*-decane, 0.004 mol% barrel, 5 mM MES, 1.3 M KCl, pH 5.0) after addition of 50 μM (b, upper trance) and 20 μM (b, lower trace) HPTS to the *cis* chamber (*trans* at ground). (c) Putative transition (dashed line) from free (high conductance) to HPTS-complexed channel **1** (low conductance); (d) putative transitions (dashed lines) between HPTS-complexed (low conductance) and free (high conductance) channel **1**.

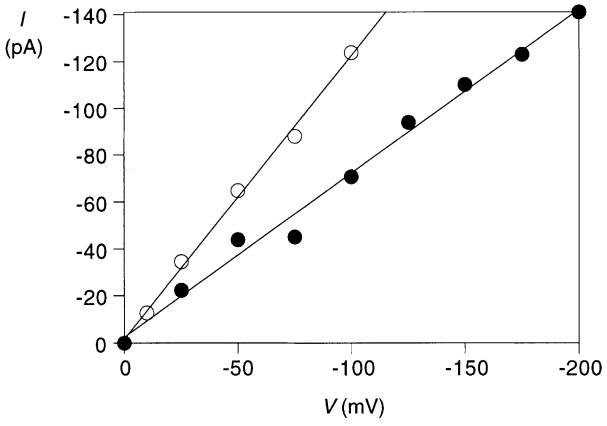

Figure 3. Single-channel I–V curves for homologous ion channels **1** (○) and **2** (●) with linear curve fit.

$$1/g = l\rho/\pi(d/2)^2 + \rho/d \qquad (1)$$

where l is the ion channel length and ρ the resistivity of the recording solution,[9–11] here $\rho = 7.716\,\Omega$cm. The length of ion channels **1** and **2** was assumed as identical with the length of the *p*-octiphenyl staves ($l = 34$ Å). The inner diameters estimated from the Hille model for labile homologue **1** and stable homologue **2** were 7.0 and 5.2 Å, respectively (Fig. 4 and Table 1). This trend was in agreement with the expected differences in the designed *p*-octiphenyl β-barrel suprastructures for expanded homologue **1** and contracted homologue **2**. Inspection of molecular models[12] suggested, however,

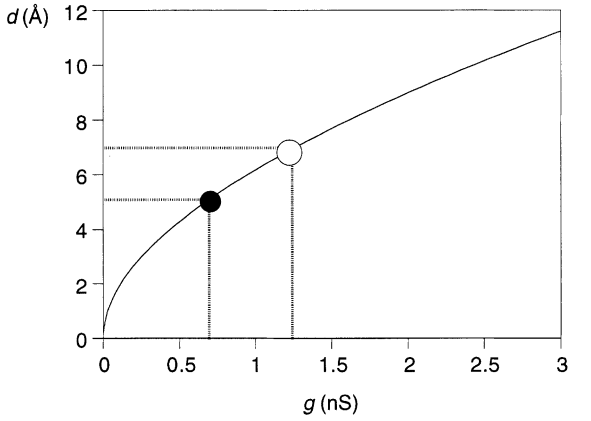

Figure 4. *d*–*g* Curve calculated for resistivity $\rho = 7.716\,\Omega$cm and ion channel length $l = 34$ Å (eq 1) with indicated *g*–*d* correlation for homologous ion channels **1** (○) and **2** (●).

Table 1. Characteristics of homologous barrels in EYPC-BLMs

Compd[a]	τ (ms)[b]	g (nS)[c]	d (Å)[d]	SCD[e]	K_D (μM)[f]	l_A (Å)[g]
1[h]	4.5	1.23	7.0	+	0.2	2.7
2[i]	>6000	0.70	5.2	–	1500	0.9

[a]See Figure 1 for designed suprastructures **1** and **2**.
[b]Single-channel lifetimes.
[c]Single-channel conductances (from I–V curves using Ohm's law).
[d]Inner channel diameter (from g using the Hille model, eq 1).
[e]Single-channel detectability of HPTS binding.
[f]Dissociation constant for HPTS at $V=0$ mV (from intercept in Woodhull plots, Fig. 7).
[g]Distance from channel entrance to site of rate-limiting HPTS association (from K_D—V curves using the Woodhull model, eq 3).
[h]Data from ref 1.
[i]This study.

that these experimentally determined inner diameters might represent underestimates by a factor of ~1.5. The observation that 5(6)-carboxyfluorescein with a minimal outer diameter of 10 Å can pass through pores formed by expanded β-barrel **1** provided experimental support in favor of internal diameters >1.4-times larger than those determined with the Hille model (unpublished results). This overall minor difference between expected and measured diameters did not come as a surprise. It is well known that the Hille model gives meaningful approximations only for cylindrical pores that are significantly larger than water and electrolytes; underestimates up to a factor of 6 are measured for small ion channels probably due reduced mobility of ions and water, particularly during ion dehydration.[11] Less dramatically reduced electrolyte mobility may well account for apparent reduction of measured diameters of homologues **1** and **2**, although their size is approaching dimensions that are compatible with the Hille approximation.

Overall satisfactory discrimination between expected diameters of homologues **1** and **2** identified the Hille model as sound method to approximate internal diameters of synthetic multifunctional pores formed by *p*-octiphenyl β-barrels. Previous results with large and 'giant' channels formed by tetrameric and hexameric *p*-octiphenyl β-barrels with internal lysines are in excellent agreement with this conclusion,[7] selected results from other synthetic ion channels as well.[13–15]

Addition of HPTS changed the single-channel characteristics of expanded homologue **1** consistently. Reduction of lifetime and conductance by HPTS with unchanged periods of ~200 ms of repetitive 'on–off' transitions were in agreement with the expected HPTS inclusion (i.e., $\tau=0.7$ ms, $g=0.7$ nS).[1] More recently, we succeeded to detect direct transitions from the characteristics of HPTS-free channels **1** (Fig. 2b) to the characteristics for barrels **1** 'filled' with HPTS (Fig. 2c) during one period of 'on–off' activity. These transitions are likely to represent HPTS entering a single channel **1**. Reduction of the HPTS concentration produced a reasonably stable low conductance level for, presumably, channels **1** with internal HPTS with occasional brief transitions to the high conductance level for HPTS-free channels **1** (Fig. 2d) during one period of 'on–off' activity. These transitions, therefore, may represent HPTS leaving and reentering a single channel **1**.

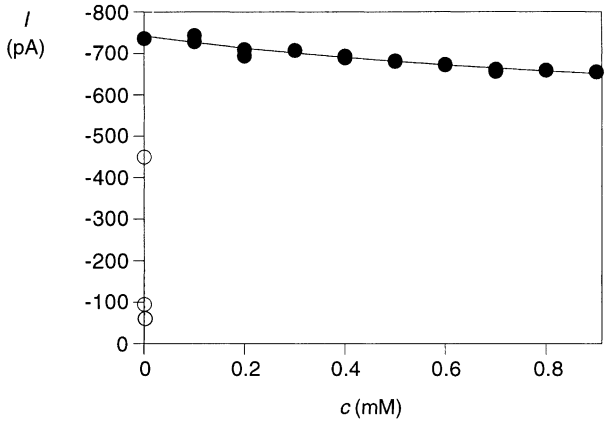

Figure 5. Multichannel dose response curves for the binding of HPTS to homologous ion channels **1** (○, data from ref 1) and **2** (●, with curve fit as solid line, eq 2) at $V=-100$ mV.

In contrast to these observations with expanded homologue **1**, the single-channel conductance of contracted homologue **2** *was not* visibly affected by the presence of up to 1 mM HPTS (Table 1). This result was in excellent agreement with the estimated difference of their inner diameters.

The current flowing across multiple channels formed by contracted homologue **2** was, however, reduced by increasing amounts of HPTS in the media (Fig. 5, ●). HPTS binding to contracted homologue **2** was orders of magnitude weaker than that to expanded homologue **1** (Fig. 5, ○). The dissociation constant K_D for HPTS binding to contracted homologue **1** at $V=-100$ mV was calculated using equation

$$(I_0 - I_\infty)/(I - I_\infty) = 1 + c(\text{HPTS})/K_D \quad (2)$$

where $I_0=-742$ pA was the multichannel current for **2** without HPTS and $I_\infty=-522$ pA that at saturation obtained from best curve fit (Fig. 6, ●, solid line).[9] This fit supports formation of a 1:1-complex.[9] A K_D (HPTS) = 1.28 mM was measured at $V=-100$ mV (Table 1). This millimolar K_D for contracted homologue **2** was more than four orders of magnitude higher than the submicromolar K_D (HPTS) = 65 nM determined previously for expanded homologue **1** at $V=-100$ mV (Table 1).

This overwhelming difference in HPTS binding by homologous *p*-octiphenyl β-barrels with internal histidines was consistent with the difference of their internal diameters identified experimentally by application of the Hille model. Namely, poor HPTS binding by contracted homologue **2**, on the one hand, was in agreement with an internal diameter smaller than HPTS. This outcome is suggestive for peripheral Cascade Blue (CB)[16] binding to terminal histidines at the mouth of channel **2** with K_D >1 mM (Fig. 6b). Submicromolar HPTS binding by

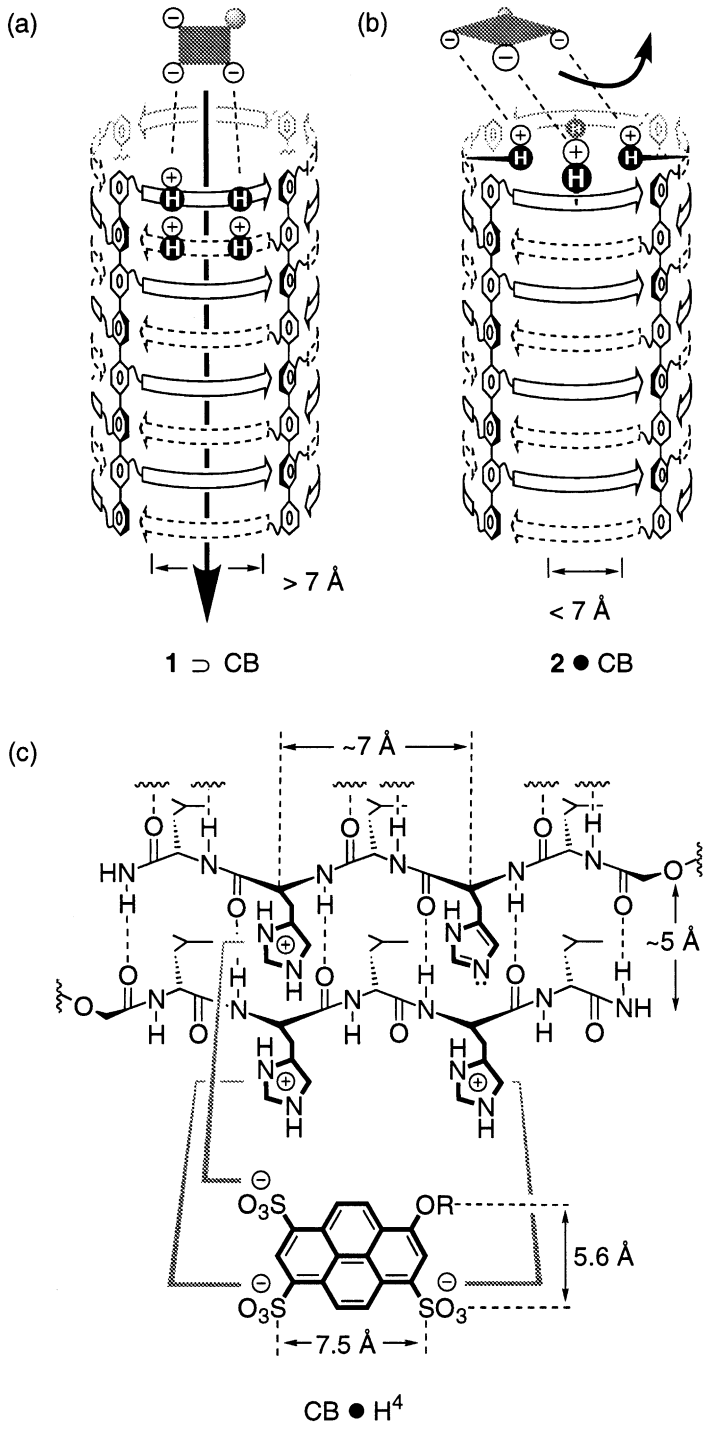

Figure 6. Proposed mechanism of CB binding to (a) internal H-quartet(s) (K_D <1 μM) in expanded homologue **1** and (b) peripheral histidines (K_D >1 mM) in contracted homologue **2**. (c) Structural detail of **1** ⊃ CB referred to as CB●H^4 recognition motif.

expanded homologue **1**, on the other hand, was in agreement with an internal diameter large enough for HPTS inclusion. This outcome, then, is supportive for internal CB binding to internal H-quartets[17] with K_D <1 μM (Fig. 6a), that is, usefulness the novel CB●H^4 recognition motif in supramolecular architecture and catalysis (Fig. 6c).

Like internal HPTS binding to expanded homologue **1** (Fig. 7, ○), peripheral HPTS binding to contracted homologue **2** was voltage dependent (Fig. 7, ●). This weak voltage dependence provided experimental evidence that, as with expanded homologue **1**, HPTS binding occurs along the ion-conducting pathway of contracted homologue **2**. According to the Woodhull equation

$$\log K_D = \log K_D(0\ \mathrm{mV}) - (l_A\ z\ F\ V)/(l\ 2.303\ R\ T) \quad (3)$$

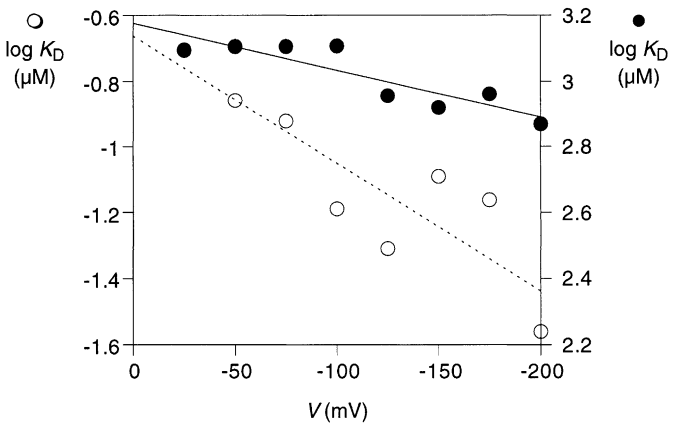

Figure 7. Woodhull plot for voltage dependence of HPTS binding to homologous ion channels **1** (○, data from ref 1) and **2** (●) with linear curve fits according to eq 3.

where $l = 34$ Å is the ion channel length, $z = -3$ the charge of HPTS at pH 5.0,[16] and F, R, and T have the usual meanings,[9,18] HPTS association rather than HPTS dissociation is the rate-limiting process with **2** (as with **1**). The Woodhull equation further revealed that the distance from the channel entrance to the HPTS binding site of contracted homologue **2** is $l_A = 0.9$ Å (Table 1). This nearly negligible value was consistent with weak peripheral HPTS binding to homologue **2** (Fig. 6b). Perhaps more importantly, the clear difference between $l_A = 0.9$ Å for contracted homologue **2** and $l_A = 2.7$ Å for expanded homologue **1** corroborated that the previous interpretation drawn from the latter value, namely association of HPTS to the first available internal H-quartet as HPTS binding site, is a meaningful one (Fig. 6a).

Esterolysis of CB-Ac to HPTS by homologues **1** and **2** was monitored following the increase in concentration of the highly fluorescent product as a function of time (Scheme 1).[1,19,20] Comparison of initial velocities of product formation suggested that, in bilayer membranes, contracted homologue **2** is 22-times less active than expanded homologue **1** (Fig. 8) and 3120-times more active than 4(5)-methylimidazole (Fig. 9).

Unlike expanded homologue **1** ($K_M = 0.7$ μM), esterolysis catalyzed by contracted homologue **2** did not approach saturation up to 4 μM substrate (Fig. 8). This indicated that substrate binding to catalyst **2** is about as poor as peripheral HPTS binding to contracted ion channel **2** (Fig. 6b), whereas substrate binding to catalyst **1** is about as good as HPTS binding within expanded ion channel **1** (Fig. 6a).

Unlike expanded homologue **1**, esterolysis by contracted homologue **2** *was* affected by the presence of bilayer membranes (Fig. 9). The observed ~50% decrease in activity in presence of small unilamellar EYPC vesicles (EYPC-SUVs) provided excellent corroborative evidence that CBs are too large to move across the contracted channel within homologue **2**, because, when bound to bilayers in transmembrane orientation, the barrel terminus located at the intravesicular bilayer interface will be inaccessible for extravesicularly added substrate. The complementary independence in esterolytic activity of expanded homologue **1** on presence or absence of EYPC-SUVs (Fig. 8) then supports that CBs are small enough to translocate across the expanded channel within homologue **1** for free access to all internal H-quartets. These insights on esterolytic activity of homologous *p*-octiphenyl β-barrels **1** and **2** are in good, indeed remarkable agreement with ion channel characteristics of **1** and **2** summarized in Table 1 and, therefore, also with their interpretation (Fig. 6).

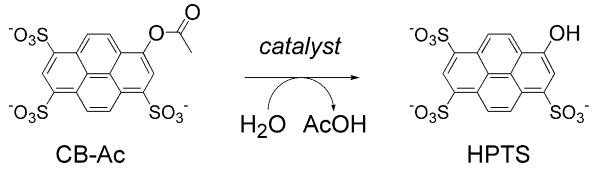

Scheme 1.

Conclusion

The bottom line is that homologous *p*-octiphenyl β-barrels **1** and **2** with esterase and ion channel activity exhibit

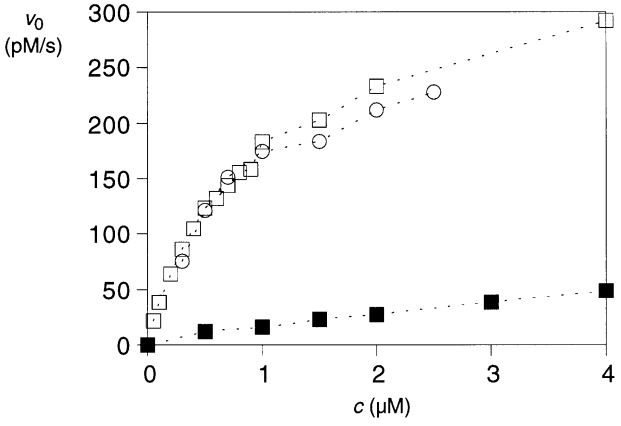

Figure 8. Initial velocity v_0 of product formation (HPTS, $\lambda_{em} = 510$ nm, $\lambda_{ex} = 415.5$ nm) as a function of substrate concentration (CB-Ac) in presence of homologous *p*-octiphenyl β-barrels **1** (○ and □, 135 nM, data from ref 1) and **2** (■, 135 nM) with (■ and □) and without (○) bilayer membranes (0.5 mM EYPC-SUVs) in 10 mM MES, 100 mM KCl, pH 5.5 at 25 °C.

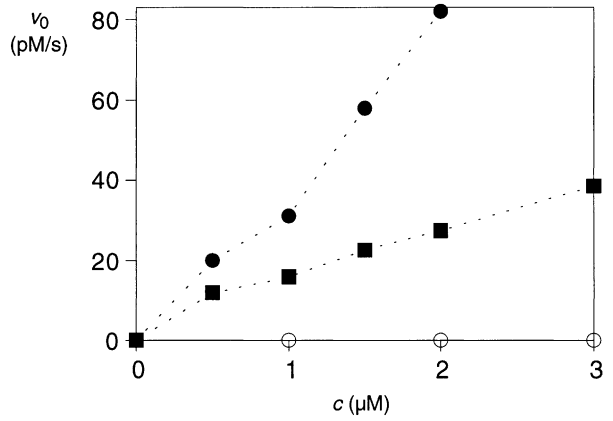

Figure 9. Initial velocity v_0 of product formation (HPTS, $\lambda_{em}=510$ nm, $\lambda_{ex}=415.5$ nm) as a function of substrate concentration (CB-Ac) in presence of *p*-octiphenyl β-barrel **2** (● and ■, 135 nM) or MeIm (○, 135 nM, data from ref 1) with (■ and ○) and without (● and ○) bilayer membranes (0.5 mM EYPC-SUVs) in 10 mM MES, 100 mM KCl, pH 5.5 at 25 °C.

complementary characteristics. Contracted homologue **2** is characterized by (a) for synthetic ion channels[13] still quite remarkable stability, (b) CB-insensitive, comparably low single-channel conductance, (c) weakly voltage-dependent, peripheral CB-binding with millimolar K_D, and (d) membrane-dependent, poor esterolytic activity. Expanded homologue **1**, in contrast, exhibits (a) poor ion channel stability, (b) CB-sensitive, comparably high single-channel conductance, (c) reasonably voltage-dependent, internal CB-binding with nanomolar K_D, and (d) membrane-independent, superb esterolytic activity.

Clearly, a small change in structure caused a big change in function. On the one hand, these complementary characteristics corroborate the mode of action proposed for expanded homologue **1**: Formation of *labile* ion channels that are large enough to permit internal CB-binding, CB-translocation, and CB-transformation (Fig. 6a and c). On the other hand, they demonstrate that homologue **2** acts differently, that is, it forms *stable* ion channels that are small enough to prevent internal CB-translocation and to promote peripheral CB-binding and CB-transformation (Fig. 6b).

Synthesis and study of the novel *p*-octiphenyl β-barrel **2** was further crucial to evaluate, in comparison with homologue **1**, methods used to characterize synthetic multifunctional pores. The results increase confidence in the validity, if used with appropriate caution, of internal diameters of synthetic pores determined from the Hille model and locations of internal active sites determined from the Woodhull equation.

Expanded homologue **1** is not sufficient for practical application in single-molecule catalysis despite superb esterolytic activity because, as illustrated with HPTS binding in Figure 2, the short lifetime of single ion channel **1** causes too much background noise for such ambitious and unprecedented experiments. Despite sufficient single-channel stability, contracted homologue **2** is not the desired 'catalytic ion channel' either because, obviously, CB binding is not detectable on the single-molecule level. One lesson learned with homologues **1** and **2** is that the key to synthetic 'catalytic ion channels' will be successful stabilization of expanded internal space as in **1**. There are three, in principle additive strategies beyond the undesired covalent barrel cross-linking, that is, increase of internal charge repulsion, increase of β-propensity, and increase of constructive barrel-membrane interactions, are currently explored in parallel.

Experimental

General

As in ref 21, supporting information, and ref 1.

$1^3,2^3,3^2,4^3,5^2,6^3,7^2,8^3$-Octa(*G*LHL-$NH_2$)-*p*-octiphenyl ($2^m$). *p*-Octiphenyl 2^m was synthesized, purified (RP-HPLC, YMC-Pack ODS-A, 250 × 10 mm, H_2O/MeOH(1% TFA) 1:4, 2 mL/min, $t_R=8.11$ min), and characterized (e.g., ESI-MS (*G*LHL-NH_2)$_8$-*p*-octiphenyl, MeOH, 1% AcOH): *m*/*z* (%) 2053 (20) $[M+2H]^{2+}$, 1369 (100) $[M+3H]^{3+}$, 1027 (40) $[M+4H]^{4+}$) following the protocol described in detail for homologue 1^m.[1]

Planar bilayer conductance. General procedures have been described in ref 1. In brief, *n*-decane containing EYPC (33 mg/mL) and 1^m or 2^m (0.016 mol%) was painted on an orifice ($d=150$ μm) separating the two chambers of a planar bilayer workstation, measured and analyzed following the protocol described (Conditions: 5 mM MES, 1.3 M KCl, pH 5.0, symmetric, agar bridge: 1 M glass KCl; electrodes: Ag/AgCl; holding potential as indicated; Bessel filter: 5 kHz; sampled at 10 kHz (**1**) and filtered at 100 Hz (**2**)). Single-channel currents *I* were obtained from histograms for different holding potentials *V* and plotted as I–V curves (Fig. 3). I–V curves were analyzed according to Ohm's law. The *g*-values obtained from linear curve fit are listed in Table 1. The Hille plot (Fig. 4) was calculated for experimental conditions following eq 1. The resistivity of the recording solution was $\rho=7.716$ Ωcm. HPTS was added to the *cis*-chamber at indicated concentrations (*trans* at ground). Macroscopic current *I* in the presence of *c* μM of HPTS was plotted against *c*, and K_D values were calculated for macroscopic dose response isotherms at $V=-20$ mV to $V=-200$ mV using eq 2. Analysis of the voltage dependence of K_D was done using the Woodhull eq 3.

Esterolysis. General procedures have been described in ref 1. In brief, 1900 μL of buffer (10 mM MES, 100 mM KCl, pH 5.5) were added into a fluorescence cuvette equipped with a magnetic stir bar and placed in a thermostatted cell holder (25°). Then, 20 μM aqueous stock solutions of CB-Ac were added to give the concentrations indicated in the v_0–*c* curves in Figures 8 and 9. Addition of 20 μL **1** or **2** (50 μM monomer in DMSO, final concentration: 500 nM monomers ≤125 nM barrels) followed. The fluorescence intensity at $\lambda_{em}=510$ nm was recorded on three channels during the

entire experiment ($\lambda_{ex} = 415.5$ nm (isosbestic point), 404 nm and 455 nm). Initial velocities of HPTS formation were obtained by comparison of the recorded intensities with experimental values for known HPTS concentrations. The reported values were confirmed to be within $\pm 5\%$ error for batch-to-batch experiments by (at least) duplicate experiments. To determine the dependence of esterolytic activity on presence and absence of bilayer membranes, small unilamellar vesicles composed of EYPC (EYPC-SUVs, 68 ± 4 nm) were prepared by dialytic detergent removal technique using a Mini Lipoprep® (AmiKa Corp) as described in ref 22. Of the resulting EYPC-SUV, suspension 50 μL (10 mM EYPC) were added before barrels in the above procedure.

Acknowledgements

We thank the Swiss NSF (21-57059.99, 2000-064818.01 and National Research Program 'Supramolecular Functional Materials' 4047-057496) for financial support.

References and Notes

1. (a) Baumeister, B.; Sakai, N.; Matile, S. *Org. Lett.* **2001**, *3*, 4229 and references therein. (b) Structural studies of barrel **1** in water: Das, G.; Ouali, L.; Adrian, M.; Baumeister, B.; Wilkinson, K. J.; Matile, S. *Angew. Chem., Int. Ed.* **2001**, *40*, 4657. (c) pH-profiles of **1**, **2**, and other barrels: Baumeister, B.; Som, A.; Das, G.; Sakai, N.; Vilbois, F.; Gerard, D.; Shahi, S. P.; Matile, S. *Helv. Chim. Acta* **2002**, *85*, 2740. (d) RNase activity of barrel **1** in water: Baumeister, B.; Matile, S. *Macromolecules* **2002**, *35*, 1549. (e) For structural aspects and molecular recognition within *p*-octiphenyl β-barrels, see: Das, G.; Onouchi, H.; Yashima, E.; Sakai, N.; Matile, S. *ChemBioChem.* **2002**, *3*, 1089. (f) Das, G.; Talukdar, P.; Matile, S. *Science* **2002**, *298*, 1600.

2. Van der Goot, F. G.; Matile, S. *Nature Biotechnol.* **2000**, *18*, 1037.

3. Mindell, J. A.; Zhan, H.; Huynh, P. D.; Collier, R. C.; Finkelstein, A. *Proc. Natl. Acad. Sci. U.S.A.* **1994**, *91*, 5272.

4. Xie, X. S.; Lu, H. P. *J. Biol. Chem.* **1999**, *274*, 15967.

5. Bayley, H.; Cremer, P. S. *Nature* **2001**, *413*, 226.

6. Tetrameric suprastructures are assumed based on previous results with **1**[1] and other barrels,[7,12] molecular models,[12] and inner diameters determined in this study; reported barrel concentrations refer to tetramers for clarity only, more direct determination of barrel stoichiometry has so far not been possible.

7. (a) Sakai, N.; Matile, S. *J. Am. Chem. Soc.* **2002**, *124*, 1184. (b) Baumeister, B.; Sakai, N.; Matile, S. *Angew. Chem., Int. Ed.* **2000**, *39*, 1955. (c) Sakai, N.; Baumeister, B.; Matile, S. *ChemBioChem.* **2000**, *1*, 123. (d) Sakai, N.; Houdebert, D.; Matile, S. *Chem. Eur. J.*, in press.

8. For comparison of dependence of barrel stability on β-sheet length with *increasing* barrel stability due to *increasing* *p*-oligophenyl length, please see: Das, G.; Matile, S. *Chirality* **2001**, *13*, 170.

9. Hille, B. *Ionic Channels of Excitable Membranes*, 2nd ed.; Sinauer: Sunderland, MA, 1992.

10. Cruickshank, C. C.; Minchin, R. F.; Le Dain, A. C.; Martinac, B. *Biophys. J.* **1997**, *73*, 1925.

11. Smart, O. S.; Breed, J.; Smith, G. R.; Sansom, M. S. P. *Biophys. J.* **1997**, *73*, 1109.

12. Baumeister, B.; Matile, S. *Chem. Eur. J.* **2000**, *6*, 1739.

13. (a) Some reviews on synthetic ion channels and pores: Gokel, G. W.; Mukhopadhyay, A. *Chem. Soc. Rev.* **2001**, *30*, 274. (b) Matile, S. *Chem. Soc. Rev.* **2001**, *30*, 158. (c) Kirkovits, G. J.; Hall, C. D. *Adv. Supramol. Chem.* **2000**, *7*, 1. (d) Sakai, N.; Matile, S. *Chem. Eur. J.* **2000**, *6*, 1731.

14. Wright, A. J.; Matthews, S. E.; Fischer, W. B.; Beer, P. D. *Chem. Eur. J.* **2001**, *7*, 3474.

15. Sanchez-Quesada, J.; Kim, H. S.; Ghadiri, M. R. *Angew. Chem., Int. Ed.* **2001**, *40*, 2503.

16. (a) CB = Cascade Blue = Pyrenyl-8-X-oxy-1,3,6-trisulfonate. Haugland, R. P. *Handbook of Fluorescent Probes and Research Chemicals*; 6th ed.; Molecular Probes, Eugene OR, 1996. (b) Whitaker, J. E.; Haugland, R. P.; Moore, P. L.; Hewitt, P. C.; Reese, M.; Haugland, R. P. *Anal. Biochem.* **1991**, *198*, 119.

17. Use of the following convention has been suggested for convenience and clarity: X^4 or X-quartet stands for four juxtaposed amino acid residues (one-letter abbreviation) on one side of a two-stranded β-sheet that form an about planar rectangle of ~ 5 Å $\times$ ~ 7 Å; example: H-quartet in Fig. 6a and c (but not b).

18. Woodhull, A. M. *J. Gen. Physiol.* **1973**, *61*, 687.

19. Wolfbeis, O. S.; Koller, E. *Anal. Biochem.* **1983**, *129*, 365.

20. For synthetic esterases, see, for example: Dugas, H. *Bioorganic Chemistry*; Springer: New York, 1996.

21. Sakai, N.; Gerard, D.; Matile, S. *J. Am. Chem. Soc.* **2001**, *123*, 2517.

22. Weiss, L. A.; Sakai, N.; Ghebremariam, B.; Ni, C.; Matile, S. *J. Am. Chem. Soc.* **1997**, *119*, 12142.